Design and Simulation of a Brushless Self-excited Air-core Compensated Pulsed Alternator

Wenhao Li, Caiyong Ye, *Member, IEEE,* Fei Xiong, Xin Liang

Abstract **— A novel brushless self-excited air-core compensated pulsed alternator (BSACPA) is presented in this paper. It consists of two sub-machines in cascade, among which one serves as an exciter and the other works as a generator. The rotor windings of the two sub-machines are connected by reverse phase sequence to realize reversal of the magnetic field. The stator windings are connected by a rectifier to realize brushless self-excited structure. As an air-core CPA of new topology, it is necessary to derive its mathematical model and carry out a comparative design. Thus, this paper focuses on the detailed design and analysis of a BSACPA prototype, which includes dimensional design and equivalent circuit establishment. Besides, the critical speed is also acquired. Accordingly, the numbers of winding coil turns are designed to increase the discharge current and power based on the theoretical analysis. Finally, the analysis and design are verified by finite-element analysis.**

Index Terms **— Brushless self-excited air-core compensated pulsed alternator (BSACPA), dimensional design, equivalent circuit.**

NOMENCLATURE

a_r	Rotor inner radius
b_r	Rotor outer radius
I_0	Rated exciter field current
I_{out}	Discharge current
$k_{\Delta n}$	Descend ratio of the rotating speed
m_{rw}	Rotor winding mass
n_r	Rotor rotating speed
Δn_r	Rotor rotating speed drop after the discharge process
n_0	Rated rotor rotating speed
t_k	Discharge duration
J_r	Rotor moment of inertia
E_r	Rotor kinetic energy storage
ΔE_r	Rotor kinetic energy storage consumption after the discharge process
P_k	Discharge power
η	Efficiency
ρ_c	Conductor resistivity
ρ_r	Rotor average density
β	Ratio of rotor axial length and outer radius
λ	Ratio of rotor inner radius and outer radius
Ω_r	Rotor angular frequency
a_{ij}	Parallel branch number
n_i	Magnetic field rotating speed
f_i	Magnetic field rotating frequency
I_{ij}	Winding current
k_{Nij}	Fundamental winding factor
k_{irs}	Coupling coefficient
l_i	Effective axial length
L_{ij}	Self-inductance per phase
$L_{ij\sigma}$	Leakage inductance per phase
m_{ij}	Phase numbers
M_i	Magnitude of mutual inductance per phase
N_{ij}	Number of coil turns per phase
p_i	Number of pole-pairs
r_{ij}	Average radius of winding
J_{ij}	Current density of winding
Q_{ij}	Joule heat of winding
R_{ij}	Resistance per phase
S_{ij}	Cross-sectional area of coil conductor
X_{ij}	Reactance per phase
Z_{ij}	Impedance per phase
τ_{ij}	Pole distance at the average radius of winding

In the above symbols, the subscripts are defined as follows: i is 1 or 2 where 1 represents the exciter and 2 represents the generator respectively. j is r or s where r represents the rotor windings and s represents the stator windings.

I. INTRODUCTION

COMPENSATED pulsed alternator (CPA, or Compulsator) is one of the most promising pulsed-power supplies for electromagnetic launchers [1]. It has been under development for decades with a wide range of configurations to improve the power density and energy density [2], [3]. The lately developed CPAs are usually air-core and multiphase [4], [5]. The brush and slip-ring mechanisms are employed to achieve self-excitation [6], [7]. However, with the characteristics of high rotating speed and large field current [8], [9], the brush and slip-ring mechanisms usually bring a number of problems such as serious wear and heat, low reliability and efficiency. Therefore, a novel brushless self-excited air-core compensated pulsed alternator (BSACPA) is proposed in this paper.

As shown in Fig.1, the connection of two sub-machines in cascade realizes the brushless structure. The left sub-machine works as a rotating-armature exciter and the right one works as a rotating-field generator. The exciter rotor winding (ERW) and generator rotor winding (GRW) are both multiphase and connected by reverse phase sequence, which is able to increase the electrical frequency of the current in the generator stator windings (GSW). The GSW is of four

This work was supported by the National Natural Science Foundation of China (Grant No.51577076).
W. Li, C. Ye, F. Xiong and X. Liang are with State Key Laboratory of Advanced Electromagnetic Engineering and Technology (AEET), School of Electrical and Electronic Engineering (SEEE), Huazhong University of Science and Technology (HUST), Wuhan, China. Corresponding author: Caiyong Ye (yecy@hust.edu.cn)

phases and double layers, which can be used to discharge as well as connect to the exciter stator winding (ESW) through a four-phase rectifier to achieve self-excitation. Because of the air-core structure, the coupling between the ESW and GSW is weak and can be ignored.

The operation steps of BSACPA are shown as follows. Firstly, the whole machine should be dragged to the rated rotating speed. Then, with the "seed-current" injected into the ESW, the exciter induces multiphase currents in the ERW. Next, the multiphase currents flow into the GRW by reverse phase sequence, function as the field current and induce four-phase currents in the GSW. After that, the four-phase currents flow back into the ESW as the exciter field current. With the cycles of the above steps, the currents in BSACPA increase exponentially, consuming the kinetic energy stored in the rotor. Finally, the GSW begins to discharge to a load when the self-excited currents reach the required value.

A novel structure with two air-core sub-machines connecting in cascade is employed in BSACPA. The designed parameters can significantly influence its final performance. Thus, it is necessary to develop its mathematical model and carry out a comparative design. In section II, its dimensional and electrical parameters are designed. In section III, the mathematical model and the self-excited condition are analyzed. In section IV, the numbers of winding coil turns of the prototype are determined. In section V, the design of BSACPA is verified by finite-element analysis.

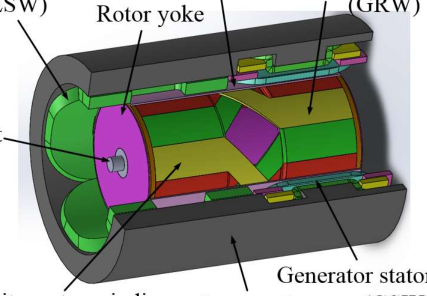

Fig.1. Three-dimensional view of BSACPA

II. Dimensional Design

The performance parameters such as the energy density and power density, mechanical parameters e.g. the line velocity of the rotor outer edge, electrical parameters including the self-inductance, mutual inductance and resistance of each winding are all closely related to the main dimensions. Thus, the first step of design should be the main dimensional design. The dimensions mainly include the inner and outer diameters of the rotor and stator yokes, the effective axial length of the rotor, the thickness and axial length of each winding, the thickness of the graphite fiber sleeve and the length of the air gap. The dimensional design of BSACPA depends on the energy storage and the peak power [10].

The energy storage can be determined by the peak power. Because the rotating speed drops after the discharge process, the formula about the descend ratio of rotating speed $k_{\Delta n}$ and the kinetic energy storage E_r can be given as:

$$\frac{\Delta E_r}{E_r} = 2\frac{\Delta n}{n} - (\frac{\Delta n}{n})^2 = 2k_{\Delta n} - k_{\Delta n}^2 \quad (1)$$

The energy consumption ΔE_r can be given as:

$$\Delta E_r = P_k \cdot t_k / \eta \quad (2)$$

The rotor kinetic energy storage E_r can be given as:

$$E_r = \frac{1}{2} J_r \Omega_r^2 = \frac{\pi^3}{3600} \rho_r \cdot \beta \cdot (1-\lambda^4) \cdot b_r^5 \cdot n^2 \quad (3)$$

β and λ are recommended by the following values [11]:

$$\begin{cases} \beta = l_r / b_r = 2.0-4.0 \\ \lambda = a_r / b_r = 0.4-0.7 \end{cases} \quad (4)$$

Assume that the target discharge power P_k is 2.5 MW, the discharge duration t_k is 4 ms, the machine efficiency η is about 50% and the rated rotor rotating speed n_0 is 20000r/min. It is expected that after a cycle of pulsed discharge process, the descend ratio of the rotating speed $k_{\Delta n}$ is not over 10%. Hence, the rotor kinetic energy storage E_r is determined to be about 100 kJ and the rotor moment of inertia J_r should be about $0.0456\ kg \cdot m^2$. The rotor yoke inner and outer diameters are designed to be 60mm and 150mm respectively and the rotor axial length is designed to be 600mm.

The thickness of the windings should be moderate. On the one hand, the winding cannot be too thin. Otherwise, the resistance will be too large, leading to the winding overheating or failing self-excitation. On the other hand, it cannot be too thick either. Because the thicker the windings are, the weaker the coupling between the field and armature windings is. The thicknesses of the rotor windings and stator windings are designed to be 5 mm and 20 mm, respectively.

The thickness of the graphite fiber sleeve should be appropriate to guarantee its tensile strength and increase the coupling between the stator and rotor windings. Similarly, the thickness of the air gap should also be suitable to ensure the safety when BSACPA works at a high rotating speed and the coupling between the stator and rotor windings. They are both designed to be 1.5 mm.

Finally, a set of dimensional parameters of the prototype is shown in Table I.

TABLE I
MAIN DIMENSIONAL PARAMETERS OF A PROTOTYPE

Symbol	Main parameters	Value
n_0	Rated rotating speed	20000 r/min
p_1	Number of pole-pairs of exciter	2
p_2	Number of pole-pairs of generator	2
d_{ri}	Inner diameter of rotor yoke	60 mm
d_{ro}	Outer diameter of rotor yoke	150 mm
l_r	Rotor axial length	600 mm
l_1	Effective axial length of the exciter	150mm
l_2	Effective axial length of the generator	150mm
d_{rw}	Thickness of rotor windings	5 mm
d_{1s}	Thickness of ESW	20 mm
d_{2s}	Thickness of GSW	10 mm
d_s	Thickness of graphite fiber sleeve	1.5 mm
δ_0	Thickness of air gap	1.5 mm
d_{si}	Inner radius of stator yoke	166 mm
d_{so}	Outer radius of stator yoke	190 mm
η_{1s}	Surface occupancy of ESW	75%
J_r	Rotational inertia of rotor	$0.0456\ \text{kg} \cdot m^2$
E_r	Kinetic energy storage of rotor yoke	100 kJ

III. Mathematical Model and Self-excited Condition

The mathematical model of BSACPA is established by analyzing its equivalent circuit. The working processes of BSACPA such as self-excitation and electrical discharge are complex. In order to simplify the analysis, only the steady state is concerned. Assuming that the field current in the ESW is constant, the discharge current in the GSW will be acquired and the relationship among the discharge current and other parameters will be obatined.

A. Electrical parameter expressions

Before the equivalent circuit is analyzed, electrical parameters such as self-inductance, mutual inductance and resistance of each winding should be deduced firstly.

Define k_{irs} as the coupling coefficient which represents the coupling strength between the field and armature windings. It is expressed as:

$$k_{irs} = (\frac{r_{ir}}{r_{is}})^{p_i} \tag{6}$$

Self-inductance per meter length L_{ij} can be expressed as:

$$L_{ij} = \frac{2\mu_0}{\pi}\frac{(N_{ij}k_{Nij})^2}{p_i} \tag{7}$$

where μ_0 is the relative permeability of vacuum.

Magnitude of mutual inductance between the rotor and stator windings at radii r_{ir} and r_{is} can be expressed as:

$$M_i = \frac{2\mu_0}{\pi}\frac{k_{1rs}(N_{ir}k_{Nir})(N_{is}k_{Nis})}{p_i} \tag{8}$$

Leakage inductance of windings can be calculated by the self-inductance and the mutual inductance:

$$L_{ir\sigma} = L_{ir} - M_i\frac{N_{ir}k_{Nir}}{N_{is}k_{Nis}} = [1-k_{irs}]L_{ir} \tag{9}$$

$$L_{is\sigma} = L_{is} - M_i\frac{N_{is}k_{Nis}}{N_{ir}k_{Nir}} = [1-k_{irs}]L_{is} \tag{10}$$

The winding resistance without considering the end winding can be expressed as:

$$R_{ij} = \frac{\rho_c N_{ij} l_i}{a_{ij} S_{ij}} \tag{11}$$

B. Single-phase equivalent circuit

The exciter can be regarded as a synchronous generator and its single-phase equivalent circuit is shown in Fig.2.

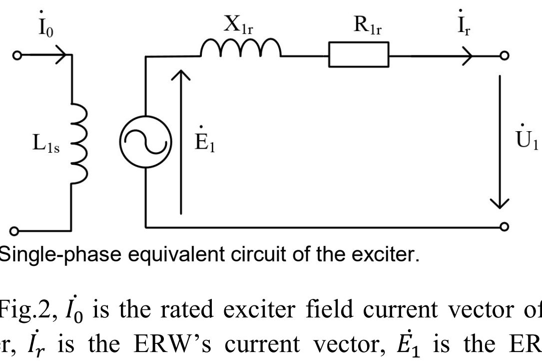

Fig.2. Single-phase equivalent circuit of the exciter.

In Fig.2, $\dot{I}_0$ is the rated exciter field current vector of the exciter, $\dot{I}_r$ is the ERW's current vector, $\dot{E}_1$ is the ERW's induced electromotive force vector, $\dot{U}_1$ is the output terminal voltage vector of the exciter.

The effective value of the ERW's induced electromotive force E_1 is given by

$$E_1 = 4k_{N1}f_1N_{1r}k_{N1r}\phi_1 \tag{12}$$

$$f_1 = p_1n_r / 60 \tag{13}$$

where k_{N1} is the exciter magnetic field waveform coefficient. ϕ_1 is the magnitude of the magnetic flux per pole and can be expressed as:

$$\phi_1 = \frac{2}{\pi}B_{1rm}\tau_{1r}l_1 \tag{14}$$

$$\tau_{1r} = \pi r_{1r} / p_1 \tag{15}$$

where B_{1rm} is the radial magnetic flux density at the average radius of the ERW.

Because the radius of the ERW r_{1r} is less than the radius of the exciter stator winding, B_{1r} can be given as [12]:

$$B_{1rm} = \frac{\mu_0 K_{1s}}{2}(\frac{r_{1r}}{r_{1s}})^{p_1-1} \tag{16}$$

where K_{1s} is the magnitude of the exciter field line current which is given as:

$$K_{1s} = \frac{2N_{1s}\cdot k_{N1s}\cdot I_0}{\pi\cdot r_{1s}} \tag{17}$$

According to (12)-(17), E_1 can be expressed as:

$$E_1 = \frac{\sqrt{2}\mu_0}{30}(N_{1r}k_{N1r})(N_{1s}k_{N1s})k_{1rs}\cdot l_1\cdot n_r\cdot I_0 \tag{18}$$

The generator can be regarded as an alternator whose rotating speed of magnetic field is larger than its mechanical rotating speed. Its single-phase equivalent circuit is shown in Fig.3.

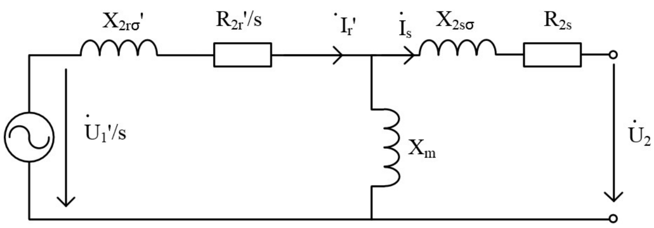

Fig.3. Single-phase equivalent circuit of the generator.

In Fig.3, $\dot{I}_s$ is the GSW's current vector and $\dot{U}_2$ is the output terminal voltage vector of the generator. The superscript in the figure represents that the parameters are under winding conversion. The parameters divided by slip ratio s means that they are under frequency conversion. The winding conversion and frequency conversion are given in (19)-(21).

$$k_e = \frac{N_{2s}k_{N2s}}{N_{2r}k_{N2r}} \tag{19}$$

$$k_i = \frac{m_{2s}N_{2s}k_{N2s}}{m_{2r}N_{2r}k_{N2r}} \tag{20}$$

where k_e is the voltage ratio and k_i is the current ratio.

$$s = \frac{n_2 - n_r}{n_2} = \frac{p_1}{p_1 + p_2} \tag{21}$$

Each parameters under winding conversion and frequency conversion can be referred to (22)-(25).

$$E' = k_eE \tag{22}$$

$$i' = i / k_i \tag{23}$$

$$R'/ s = k_ek_iR / s \tag{24}$$

$$X' = k_ek_i\omega_1L \tag{25}$$

X_m is the generator excited reactance and its magnitude is given as:

$$X_m = \omega_1k_eM_2 \tag{26}$$

Combining the equivalent circuits of the exciter and generator, the single-phase equivalent circuit of BSACPA can be obtained, as shown in Fig.4.

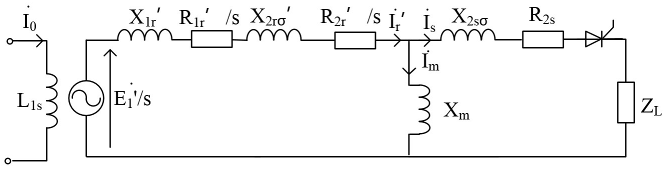

Fig.4. Single-phase equivalent circuit of BSACPA.

Assuming that the load and the winding resistances are ignored, the magnitude of the discharge current deduced from Fig.4 can be expressed as:

$$I_{out} = \frac{k_{1rs}k_{2rs}\dfrac{N_{1r}k_{N1r}}{N_{2r}k_{N2r}}}{\dfrac{m_{2s}}{m_{2r}}(\dfrac{N_{1r}k_{N1r}}{N_{2r}k_{N2r}})^2 + (\dfrac{m_{2s}}{m_{2r}} + k_{2rs})(1-k_{2rs})\dfrac{p_1}{p_2}\dfrac{l_2}{l_1}} \cdot \frac{N_{1s}k_{N1s}}{N_{2s}k_{N2s}} \cdot I_0 \quad (27)$$

C. Four-phase equivalent circuit

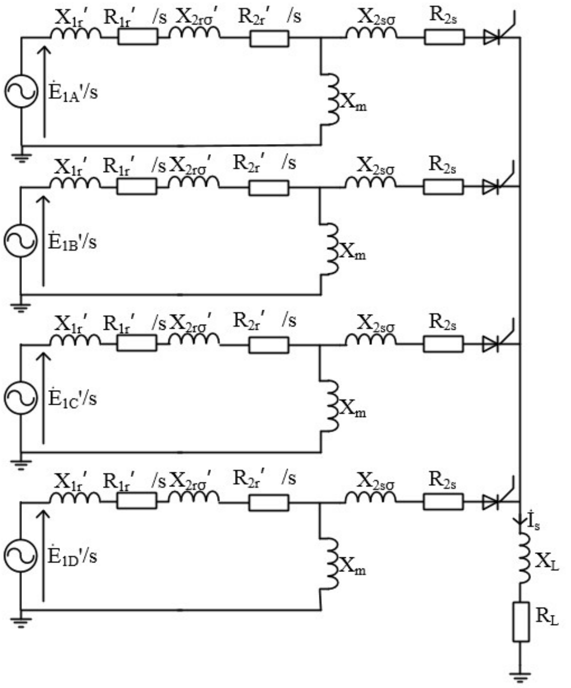

Fig. 5. Four-phase equivalent circuit of BSACPA.

In the four-phase equivalent circuit, the four-phase rectification, the commutation voltage loss, the stator winding resistances and the load resistance are all taken into consideration while the rotor winding resistances are ignored. Analyze the four-phase equivalent by Thevenin's theorem, the discharge current I_{out} can be expressed as:

$$I_{out} = \frac{4}{\pi}U_{oc} / (\frac{4}{\pi}R_{in} + \frac{2}{\pi}X_{in} + R_L) \quad (28)$$

where U_{oc} is the no-load voltage, R_{in} is the internal resistance, X_{in} is the internal reactance and R_L is the load resistance. U_{oc}, R_{in} and X_{in} are given in (29)-(31).

$$U_{oc} = \frac{E_1'}{s} \cdot \frac{jX_m}{\dfrac{R_{1r}'}{s} + \dfrac{R_{2r}'}{s} + j(X_{1r}' + X_{2r\sigma}' + X_m)} \quad (29)$$

$$R_{in} = R_{2s} \quad (30)$$

$$X_{in} = X_{2s\sigma} + \frac{X_m(X_{1r}' + X_{2r\sigma}')}{(X_m + X_{1r}' + X_{2r\sigma}')} \quad (31)$$

D. Verification and discussion

The equivalent circuits is verified by the finite-element analysis (FEA), as shown in Fig.6. Each figure only changes one parameter while the other parameters are constant. The conditions for the above pictures are shown as follows:

(a) N_{2s}=20, N_{1r}=2, N_{2r}=2, n_r=20000 r/min, I_0=10 kA when N_{1s} changes.

(b) N_{1s} =100, N_{1r}=2, N_{2r}=2, n_r=20000 r/min, I_0 =10 kA when N_{2s} changes.

(c) N_{1s} =100, N_{2s} =20, N_{2r}=20, n_r=20000 r/min, I_0=10 kA when N_{1r} changes.

(d) N_{1s} =100, N_{2s}=20, N_{1r}=20, n_r=20000 r/min, I_0=10 kA when N_{2r} changes.

(e) N_{1s} =100, N_{2s}=20, N_{1r}=2, N_{2r}=2, I_0=10 kA when n_r changes.

(f) N_{1s} =100, N_{2s}=20, N_{1r}=2, N_{2r}=2, n_r=20000 r/min when I_0 changes.

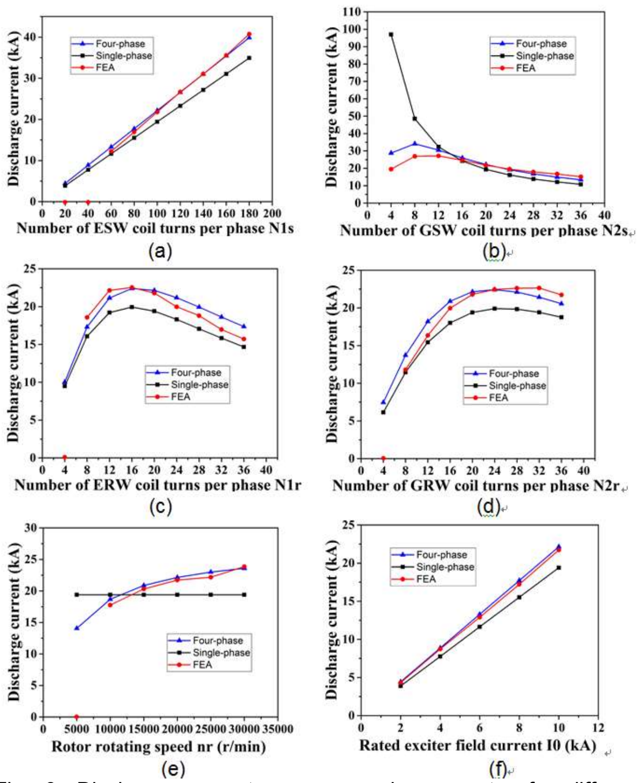

Fig. 6. Discharge currents versus each parameter for different analytical methods.

It can be seen from Fig.6 that the curves of FEA are more close to those of the four-phase equivalent circuit, which means the four-phase equivalent is more accurate than the single-phase equivalent circuit. It is because that the single-phase equivalent circuit is just a simplified model, ignoring the four-phase rectification and all the winding resistances. However, the relationships among the discharge current and each parameter can be determined generally from (27), which is deduced from the single-phase equivalent. The relationships can be concluded as follows:

1) The value of I_{out} is proportional to the number of effective coil turns of the ESW N_{1s} while it is inversely proportional to the number of effective coil turns of the GSW N_{2s}.

2) There are certain numbers of effective coil turns of the ERW N_{1r} and GRW N_{2r} making the value of I_{out} largest.

3) The value of I_{out} increases slightly with the increase of the rotor rotating speed n_r.
4) The value of I_{out} is proportional to the rated exciter field current I_0.

In conclusion, the mathematical model of the equivalent circuits and above rules can provide a guidance to the optimization of BSACPA parameters.

E. Self-excited condition

As shown in Fig.6, there are several zero points on the curve of FEA. It is because that the machine at these points is not able to self-excite. Whether BSACPA can work successfully is primarily decided by whether it is self-excited. Thus, it is important to determine the self-excited condition and obtain the value of the critical rotating speed.

Assume that the exciter field current is i_0^- at the time t_0^- and it will produce a discharge current i_{out} in the GSW at the time t_0^+. If the condition $i_{out} > i_0^-$ is satisfied, the currents in the machine will rise exponentially and BSACPA is able to self-excite.

Thus, according to the formulas (28)-(31), the critical self-excited rotating speed n_e is given as:

$$n_e = \frac{k_{st}\cdot 15\cdot(4/\pi\cdot R_{2s}+R_{1s})}{(p_1+p_2)[\sqrt{2}k_e M_1\frac{L_m}{L_m+L_{1r}'+L_{2r\sigma}'}-(L_{2s\sigma}+\frac{L_m\cdot(L_{1r}'+L_{2r\sigma}')}{L_m+L_{1r}'+L_{2r\sigma}'})]} \quad (32)$$

k_{st} is the correction coefficient, which is associated with the phase number, the current frequency and the filter inductance.

IV. Determination of Numbers of Winding Coil Turns

In section III, it can be found that the discharge current is closely relevant to the number of effective coil turns of each winding, the rotor rotating speed and the rated exciter field current. Thus, the numbers of winding coil turns can be designed to significantly improve the performance of BSACPA. In this paper, the goal of coil turns number design is to ensure the successful work as well as to improve the discharge current and power as much as possible. The machine works under the constant condition of the rated rotating speed (20000 rpm), the main sizes (Table I), the load impedance (10 mΩ) and the filter inductance (10 μH) .

(27) can be simplified as follows:

$$I_{out} = \frac{k_{1rs}k_{2rs}k_{Nr}k_{Ns}}{k_m k_{Nr}^2+(k_m+k_{2rs})(1-k_{2rs})k_p/k_l}\cdot I_0 \quad (33)$$

where k_{Nr} is the ratio of $N_{1r}k_{N1r}$ and $N_{2r}k_{N2r}$, k_{Ns} is the ratio of $N_{1s}k_{N1s}$ and $N_{2s}k_{N2s}$, k_m is the ratio of m_{2s} to m_{2r}, k_p is the ratio of p_1 to p_2 and k_l is the ratio of l_1 to l_2.

When the topology and dimensions of BSACPA have been determined, k_m, k_p and k_l are determined as well. Thus firstly we should determine the values of k_{Nr} and k_{Ns} with the more accurate four-phase equivalent circuit.

In Fig.7, the green curve with square symbol illustrates that when N_{2r} is a constant (100), the discharge current peaks at 22.435 kA when N_{1r} is 84. The other three lines shows that the discharge current is constant if k_{Nr} does not change. In addition, the discharge current does not change a lot when k_{Nr} is around 1. As a result, taking the practical craft into consideration, the value of k_{Nr} is taken to be 1, and the values of N_{1r} and N_{2r} are both 2 to increase the winding

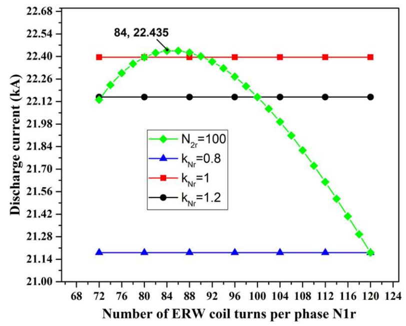

Fig. 7. Discharge current versus windings coil turns number of ERW.

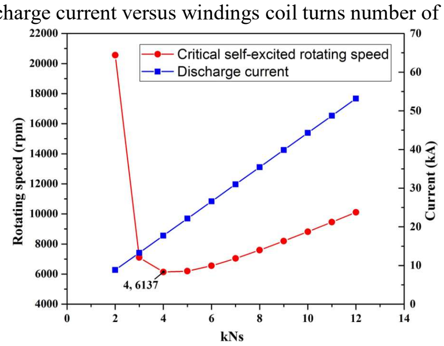

Fig.8. Discharge current and critical self-excited rotating speed versus k_{Ns}.

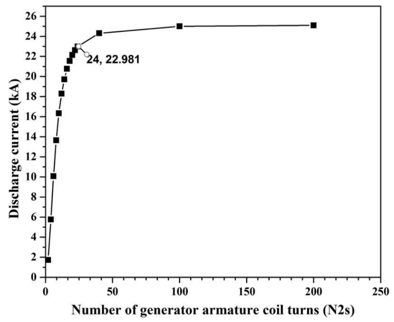

Fig.9. Discharge current versus N_{2s} when k_{Ns} is 5.

effective cross-section area.

In Fig. 8, N_{2s} equals to a constant of 20 and N_{1s} varies from 20 to 120. The blue curve with square symbol illustrates that the discharge current is proportional to k_{Ns}. The critical rotating speed reaches the minimum value (6137 r/min) when k_{Ns} is 4. When k_{Ns} is larger than 4, the critical self-excited rotating speed increases, which means that the self-excitation becomes more difficult. When the critical self-excited rotating speed becomes larger than the rated rotor rotating speed, the self-excitation fails and the machine cannot successfully work. Thus, the value of the discharge current and the critical self-excited rotating speed should be considered synthetically.

In terms of this prototype, k_{Ns} is determined to be 5. Once k_{Ns} is confirmed, the relationship between discharge current and N_{2s} is shown in Fig.9. From the picture, we can see that the amount of discharge current experiences a rise steadily first but then gradually levels off with the value of N_{2s} growing. It results from the internal resistance of the generator armature winding. As a result, the value of N_{2s} takes 24 and N_{1s} takes 120 correspondingly.

In addition, after the number of each winding coil turns is determined, the temperature rise should be taken into consideration and checked. Because BSACPA works in an instantaneous operation, the heat energy produced by the windings is difficult to transfer to the surrounding environment in such a short time (milliseconds level). Thus, the Joule heat is assumed to be thoroughly used to increase the temperature of the conductor [10]. Ref. [13] gives a minimum cross-sectional area to limit the temperature rise of the windings, as shown in (34).

$$S_a = I\sqrt{\frac{\alpha \cdot \rho_0 \cdot t}{\rho_m \cdot c \cdot \ln(\frac{1+\alpha\theta_k}{1+\alpha\theta_0})}} \quad (34)$$

where I is the rms of the winding current, t is the time current exists, ρ_0 is the resistivity of the conductor at 0°C, α is the temperature coefficient of winding conductor, ρ_m is the mass density of armature winding conductor, c is the heat capacity ratio of conductor, θ_k is the winding temperature after discharge, and θ_0 is the winding initial temperature.

Finally, the performance and electrical parameters of BECPA are shown in Table II.

TABLE II
ANALYTICAL PERFORMANCE AND ELECTRICAL PARAMETERS OF BSACPA

Symbol	Value	Symbol	Value
N_{1s}	120	N_{2s}	24
N_{1r}	2	N_{2r}	2
L_{1s}	518.14 μH	L_{2s}	27.30 μH
L_{1r}	0.24 μH	L_{2r}	0.24 μH
M_1	7.91 μH	M_2	1.80 μH
$L_{1s\sigma}$	128.00 μH	$L_{2s\sigma}$	6.94 μH
$L_{1r\sigma}$	0.08 μH	$L_{2r\sigma}$	0.08 μH
R_{1s}	19.14 mΩ	R_{2s}	2.30 mΩ
R_{1r}	0.06 mΩ	R_{2r}	0.06 mΩ
k_e	11.31	k_i	7.54
ω_2	8377.58 rad/s	s	0.50
I_0	10.00 kA	I_{out}	22.98 kA
R_L	10.00 mΩ	P_{out}	5.28 MW

V. FINITE-ELEMENT ANALYSIS

The above designs are verified by the 2D finite-element analysis in order to save time and resource. The corresponding simulation model of the BSACPA prototype is shown in Fig.10.

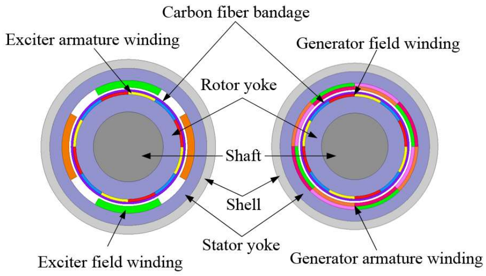

Fig. 10. Simulation model of BSACPA prototype.

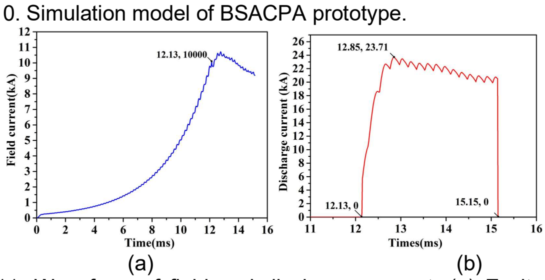

(a) (b)

Fig. 11. Waveform of field and discharge current. (a) Exciter field current. (b) Discharge current.

In terms of the designed dimensional parameters, the field current and discharge current are shown in Fig.11. Fig.11 (a) shows the field current rises exponentially until the end of self-excitation at 12.13 ms. Fig.11 (b) illustrates the discharge current ascends in a very short time. The peaking current is about 23.71 kA at 12.85 ms, which is only differed from the analytical value by 3% relative error. The peak power can reach about 5.6 MW accordingly.

In conclusion, the results of the simulations prove the validity of the design.

VI. CONCLUSION

In this paper, the structure of BSACPA is introduced and a set of dimensional parameters of a prototype are designed step by step. Then, a simplified mathematical model is presented. The analytical method of combining two equivalent circuits can be applied to other similar cascaded electrical machines. Besides, self-excited condition, the essential factor of successful self-excitation is obtained accordingly. Moreover, the determination of numbers of winding coil turns provides a complete process and solution to enhance the performance of BSACPA. Conclusively, this paper presents a detailed design process of a BSACPA prototype, which can also provide a guidance to other CPAs' design.

VII. REFERENCES

[1] C. Ye, J. Yang, X. Liang and W. Xu, "Design and research of a high-speed and high-frequency pulsed alternator," in *IEEE Trans. Plasma Sci.*, vol. 45, no. 7, pp. 1512-1518, July 2017.

[2] J. R. Kitzmiller et al., "Predicted versus actual performance of the model scale compulsator system," *IEEE Trans. Mag.*, vol. 37, no. 1, pp. 362-366, Jan 2001.

[3] X. Liang, et al., "Research of a novel multidisk axial flux compensated pulsed alternator," *IEEE Trans. Appl. Supercond.*, vol. 28, no. 3, pp. 1-6, April 2018.

[4] S. Wu, W. Zhao, S. Wang and S. Cui, "Overview of pulsed alternators," in *IEEE Trans. Plasma Sci.*, vol. 45, no. 7, pp. 1078-1085, July 2017.

[5] J. R. Kitzmiller, S. B. Pratap and M. D. Driga, "An application guide for compulsators," *IEEE Trans. Mag.*, vol. 39, no. 1, pp. 285-288, Jan. 2003.

[6] S. Wu, S. Cui and W. Zhao, "Design and analysis of a high-speed permanent magnet compensated pulsed alternator," *IEEE Trans. Plasma Sci.*, vol. 45, no. 7, pp. 1314-1320, July 2017.

[7] Y. Cheng, P. Yuan, C. Kan, L. Chen and Y. He, "Design and simulation of a new brushless doubly-fed pulsed alternator for high-energy pulsed lasers," *IEEE Trans. Plasma Sci.*, vol. 45, no. 7, pp. 1115-1121, July 2017.

[8] C. Ye, K. Yu, Z. Lou, Z. Ren and Y. Pan, "Investigation of pulse excitation in air-core pulsed-alternator system," *IEEE Trans. Plasma Sci.*, vol. 39, no. 1, pp. 342-345, Jan. 2011.

[9] C. Ye, K. Yu, Z. Lou and Y. Pan, "Investigation of self-excitation and discharge processes in an air-core pulsed alternator," *IEEE Trans. Mag.*, vol. 46, no. 1, pp. 150-154, Jan. 2010.

[10] Q. Zhang, S. Wu, C. Yu, S. Cui and L. Song, "Design of a model-scale air-core compulsator," *IEEE Trans. Plasma Sci.*, vol. 39, no. 1, pp. 346-353, Jan. 2011.

[11] C. Ye, K. Yu, H. Zhang, L. Tang and X. Xie, "Optimized design and simulation of a GW-scale multiphase air-core pulsed alternator," 2014 17th International Symposium on Electromagnetic Launch Technology, La Jolla, CA, 2014, pp. 1-5.

[12] C. Ye, K. Yu, H. Zhang, L. Tang and X. Xie, "Optimized design and simulation of an air-core pulsed alternator," *IEEE Trans. Plasma Sci.*, vol. 43, no. 5, pp. 1405-1409, May 2015.

[13] K. Zheng, "Research of permanent passive compulsator," M.S. thesis, Huazhong Univ. Sci. Technol., Wuhan, China, Apr., 2004